Renewable and Sustainable Energy Reviews 73 (2017) 695–705

Contents lists available at ScienceDirect

Renewable and Sustainable Energy Reviews

journal homepage: www.elsevier.com/locate/rser

Green science: Independent building technology to mitigate energy, environment, and climate change

Md. Faruque Hossain[a,b,*]

[a] Green Globe Technology, 4323 Colden Street 15L, Flushing, New York 11355, USA
[b] Department of Civil and Urban Engineering, New York University, 6 Metrotech Center, Brooklyn 11201, New York, USA

ARTICLE INFO

Keywords:
PV energy
In-Situ water supply
Biogas production
Climate change mitigation

ABSTRACT

All residential and commercial buildings are connected to conventional electricity, gas, and water supply lines to meet their vital needs, which causes severe environmental crises. Therefore, a green science application is proposed in this article to meet the total energy, water, and gas demands for a building, which can be produced by the building itself without any outside connections and is also 100% clean. To meet 100% of the energy demands of a building, a design theory is implemented wherein at least 25% of the exterior curtain wall skin and roof is used as a blackbody assisted photovoltaic (PV) panel to capture solar energy and convert it to electricity. The domestic water supply is provided by in-house treatment processes (filtration, chlorination, UV treatment and purification) from in-situ groundwater extraction by PV-panel-assisted pumping. Subsequently, the domestic waste undergoes a transformation process wherein sludge, consisting mainly of human feces, is collected in a closed anaerobic detention tank in a cellar and introduced into a bioreactor, enabling the production of biogas by *methanogenesis*; this biogas is then stored and used for cooking and HVAC equipment. Finally, the separated wastewater is treated in the cellar by applying primary, secondary, and tertiary processes and is then used for gardening, irrigation, and landscaping. The combination of these technologies, wherein a building can produce electricity, water, and gas without outside connections, is a major scientific innovation expected to dramatically mitigate the global energy, environmental, and climate change crises.

1. Introduction

Buildings have a significant impact on climate change since they account for almost 40% of energy consumption due to burning fossil fuels [1,2]. To estimate how much energy this represents, let us calculate the value based on annual global energy consumption: world energy consumption in the year 2015 was 5.59×10^{20} J (559 EJ), and nearly 2.236 EJ was consumed by residential and commercial buildings, producing nearly 8.01×10^{11} t CO_2 (218 gtC from construction out of a global total of 545 gtC; 1 gtC=10^9 t C=3.67 gt CO_2) [2]. The amount of energy used by buildings continues to increase due to the new development is occurring rapidly throughout the world. Energy consumption by buildings will continue to increase until buildings can be designed to produce sufficient renewable energy through sophisticated technology. Interestingly, light emitted by the Sun that reaches Earth is one of the most plentiful renewable energy resources [3,4]. The deployment of solar technology must come with clear and defined requirements to ensure that reliable photovoltaic (PV) systems are implemented [5]. Recent research conducted by Anish Mode et. at and presented a thorough numerous literature review on solar energy based electricity, and heat and power production as a renewable energy source [39]. Another study performed by Huihui et. at to investigate the biogas production from wastewater obtained from HTL of straw for bio-crude production, with focuses on the analysis of the microbial communities and characterization of the organics where they found methane yield production is reasonable to utilize it as an energy source [44]. Though several research has been performed to convert solar energy into electricity energy, biogas production from the *methonegenis*, but no research has been conducted as a combined effort to produce solar, gas, and water by an building itself to meet its total energy, gas, and water demand.

Thus, the present research conduction on combined technology application (energy, gas, water) for confirming a zero-emission building (ZEB). It will indeed be the highly innovative technology to balance its energy demands if the building's skin and roof are designed with at least 25% blackbody-assisted PV panels to capture solar energy to meet its total energy demand, which will reduce emissions by 8.01×10^{11} t CO_2 per year [2,6]. It is estimated that 402 ppm CO_2 is currently

* Corresponding author.
E-mail address: faruque55@aol.com.

http://dx.doi.org/10.1016/j.rser.2017.01.136
Received 29 May 2016; Received in revised form 10 December 2016; Accepted 19 January 2017
Available online 03 February 2017

present in the atmosphere, causing global warming; this must be reduced to 300 ppm CO_2 to achieve global cooling at a comfortable rate [7,8]. The use of blackbody-assisted PV panels in each building will eliminate 40% of CO_2 production per year. Interestingly, it will take only $\{\int_{300}^{402}(1-0.4)dx\}$ =61.2 years to cool the atmosphere, resulting in the reversal of climate change after 62 years.

It is well known that water reservoirs play a significant role in the Earth's ecosystem and may contribute to changes in Earth's climate once they become stratified due to water extraction for domestic water supplies [9]. Subsequently, reservoirs warm and generate methane, a greenhouse gas, in the bottom layers that are anoxic (i.e., they lack oxygen), leading to the degradation of biomass through anaerobic processes. In some cases, where flooded basins are wide and biomass volumes are high, the amount of biomass converted to methane results in a pollution potential 3.5 times greater than that of an oil-fired power plant for the same generation capacity. Methane gas is one of the most significant contributors to global climate change [1,9]. It is costly to use reservoir water treatment, supply, and maintenance of city water lines to supply each building to meet our daily water demands. Since groundwater is available within the 200 m energy line everywhere in the world and is mostly purified by natural processes by aquifers, it can be pumped and further treated at a low cost on-site to meet a building's water demand without harming the climate.

The use of a biochemical platform for the production of biofuels (ethanol) and value-added compounds (antioxidants) from grain and tree-pruning as feedstock has been studied by several researchers in the past, but it was found that the production of grain-based and/or tree-pruning bioenergy can have detrimental consequences for soil carbon sequestration, nitrous oxide emissions, nitrate pollution, biodiversity and human health [10–12] and that domestic waste is the best option to produce biogas. Thus, in this research, building domestic waste, including wastewater, that can be collected in a closed detention tank and then separated into two different chambers (for wastewater and feces) was chosen. For context, a person produces 0.4–0.5 kg/day of human feces (solid waste), which can produce 0.4 m^3 biogas/day, which can cook three meals per day for a family of four [44]. Treated wastewater can be used for rooftop gardening and for a building's landscape irrigation. It would truly be an independent building technology that can meet all of its energy, water, gas demands; thus, this capability is expected to play a key role in reducing climate change.

2. Methods and materials

2.1. PV array modeling

In this article, a mathematical model is analyzed that describes the operation and behavior of a PV generator in which the maximum power output can be calculated for a module once the PV solar irradiance on the PV module and temperature is determined [13]. Interestingly, the model can be simplified in terms of the maximum power output, which has a reciprocal relationship with the temperature module and a logarithmic relationship with the solar radiation absorbed by the PV module [14–16]. This model, with the associated calculation procedures, accuracy and parameters of a current–voltage relationship, is presented in Fig. 1) and in more detail in the single-diode equivalent circuit of a PV cell model module (Fig. 2 and 3).

with $I_{pv\text{-}sim}$ is calculated from the model with a diode, using a wide range of variation of the illumination received by the photovoltaic p.

$I_{pv\text{-}sim}$ is calculated based on a model with a diode, using a wide range of variation in the illumination received by the PV panel; p contains various parameters to determine P_1, P_2, P_3, P_4, A, R_s, and R_{sh} and was therefore used as the control for the minimal control strategy to simultaneously achieve a green active and reactive power source with active filtering capability [15,17].

The power output of a PV array is based on solar irradiance and ambient temperature; thus, the model is calculated as follows:

$$P_{pv} = \eta_{pvg} A_{pvg} G_t, \tag{1}$$

where η_{pvg} is the PV generation efficiency, A_{pvg} is the PV generator area (m^2), and G_t is the solar radiation in a tilted module plane (W/m^2). The parameter η_{pvg} is further defined as

$$\eta_{pvg} = \eta_r \eta_{pc}[1 - \beta(T_c - T_{cref})], \tag{2}$$

where η_{pc} is the power conditioning efficiency, which is equal to one when MPPT is used; β is a temperature coefficient (0.004–0.006 per °C); η_r is the reference module efficiency; and T_{cref} is the reference cell temperature in units of °C. The reference cell temperature (T_{cref}) can be obtained from the relation

$$T_c = T_a + \left(\frac{NOCT-20}{800}\right) G_t, \tag{3}$$

where T_a is the ambient temperature in °C, NOCT is the nominal operating cell temperature in °C, and G_t is the solar radiation in a tilted module plane (W/m^2). The total radiation in the solar cell, considering both normal and diffuse solar radiation, can be estimated as

$$I_t = I_b R_b + I_d R_d + (I_b + I_d) R_r \tag{4}$$

The solar cell, which is the building block of the solar array, is essentially a P-N junction semiconductor capable of producing electricity via the PV effect [18–20]. PV cells are interconnected in a series-parallel configuration to form a PV array, and graphene is integrated in the PV module to improve the efficiency of the resulting PV device [16,21].

Using an ideal single diode, as shown in Fig. 2, for an array with N_s series-connected cells and N_p parallel-connected cells, the array current can be related to the array voltage as follows:

$$I = N_p\left[I_{ph} - I_{rs}\left[\exp\left(\frac{q(V + IR_s)}{AKTN_s} - 1\right)\right]\right], \tag{5}$$

where

$$I_{rs} = I_{rr}\left(\frac{T}{T_r}\right)^3 exp\left[\frac{E_G}{AK}\left(\frac{1}{T_r} - \frac{1}{T}\right)\right] \tag{6}$$

and q is the electron charge (1.6×10^{-9} C), K is Boltzmann's constant, A is the diode ideality factor, and T is the cell temperature (K). I_{rs} is the cell reverse saturation current at T, T_r is the cell reference temperature, I_{rr} is the reverse saturation current at T_r, and E_G is the band gap energy of the semiconductor used in the cell. The photo current I_{ph} varies with the cell's temperature and radiation as follows:

$$I_{ph} = \left[I_{SCR} + k_i(T - T_r)\frac{S}{100}\right], \tag{7}$$

where I_{SCR} is the cell short-circuit current at the reference temperature and radiation, k_i is the short-circuit current temperature coefficient, and S is the solar radiation (mW/cm^2). The single-diode model includes an additional shunt resistance in parallel to the ideal shunt diode model. The *I-V* characteristics of the PV cell can be derived using a single-diode model as follows:

$$I = I_{ph} - I_D \tag{8}$$

$$I = I_{ph} - I_0\left[\exp\left(\frac{q(V + R_s I)}{AKT} - 1\right) - \frac{V + R_s I}{R_{sh}}\right], \tag{9}$$

where I_{ph} is the photo current (A), I_D is the diode current (A), I_O is the inverse saturation current (A), A is the diode constant, q is the charge of the electron (1.6×10^{-9} C), K is Boltzmann's constant, T is the cell temperature (°C), R_s is the series resistance (Ω), R_{sh} is the shunt resistance (Ω), I is the cell current (A), and V is the cell voltage (V). The output current of the PV cell, using the diode model, can be described as follows [20,22,23]:

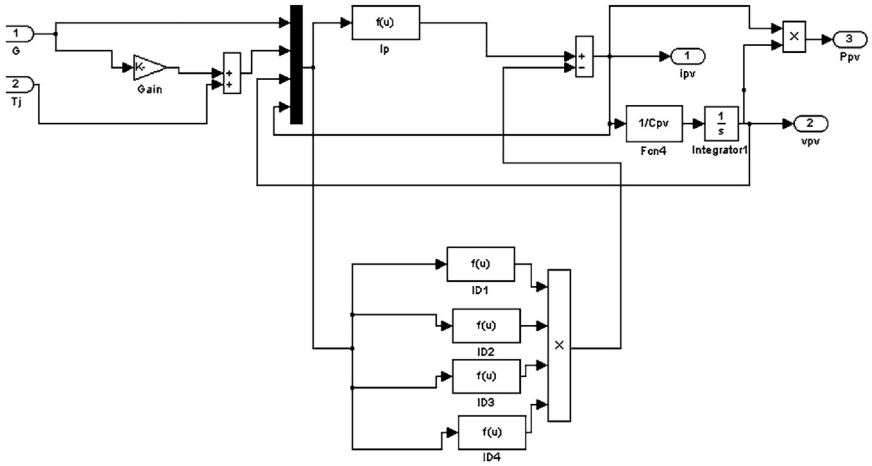

Fig. 1. Diagram of PV System Model.

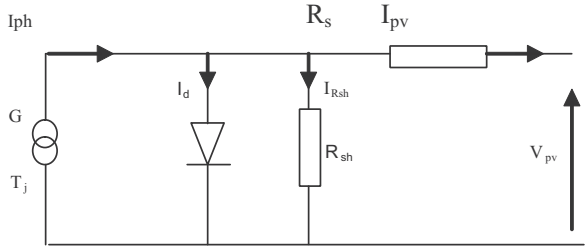

Fig. 2. Single-diode equivalent circuit of a PV cell model module or array as a continuous function for a given set of operating conditions.

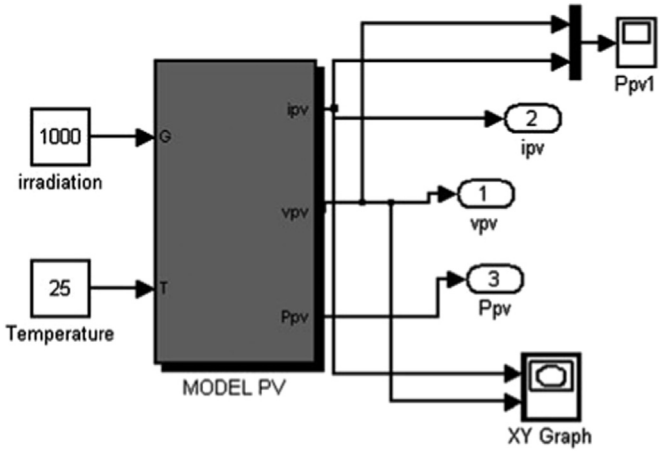

Fig. 3. Activated Bloc diagram of the PV model.

$$I=I_{PV}-I_{D1}-I_{D2}-\left(\frac{V+IR_S}{R_{SH}}\right), \tag{10}$$

where

$$I_{D1}= \quad I_{01}\left[\exp\left(\frac{V+IR_s}{a_1V_{T1}}\right)-1\right], \tag{11}$$

$$I_{D2}= \quad I_{02}\left[\exp\left(\frac{V+IR_s}{a_2V_{T2}}\right)-1\right], \tag{12}$$

where I_{O1} and I_{O2} are the reverse saturation currents of diode 1 and diode 2, respectively, and V_{T1} and V_{T2} are the thermal voltages of the respective diodes. The diode ideality constants are represented by a_1 and a_2, respectively. The simplified model of the PV system model is as follows:

$$v_{oc}=\frac{V_{oc}}{cKT/q} \tag{13}$$

$$P_{max}=\frac{\frac{V_{oc}}{cKT/q}-\ln\left(\frac{V_{oc}}{cKT/q}+0.72\right)}{\left(1+\frac{V_{oc}}{nKT/q}\right)}\left(1-\frac{V_{oc}}{\frac{V_{oc}}{I_{SC}}}\right)\left(\frac{V_{oc0}}{1+\beta\ln\frac{G_0}{G}}\right)\left(\frac{T_o}{T}\right)^{y}I_{sc0}\left(\frac{G}{G_o}\right)^{a}, \tag{14}$$

where v_{oc} is the normalized value of the open-circuit voltage V_{oc} with respect to the thermal voltage $V_t=nkT/q$, n is the ideality factor ($1<n<2$), K is the Boltzmann constant, T is the PV module temperature in K, q is the electron charge, α is the factor responsible for all the non-linear effects upon which the photocurrent depends, β is a PV module technology-specific dimensionless coefficient, and γ is the factor representing all the non-linear temperature-voltage effects. Eq. (14) represents the maximum power output of a single PV module. A real system consists of multiple PV modules connected in series and in parallel. The total power output for an array with N_s cells connected in series and N_p cells connected in parallel with power P_M for each module is

$$P_{array}=N_sN_pP_M \tag{15}$$

2.2. Design of a solar panel

The new century was marked by a growth in PV in terms of both research and market expansions [21]. So far, the PV mechanism, i.e., the conversion of sunlight into electricity, has been dominated by linking solid-state devices often made of silicon. However, this domain is now being challenged by the emergence of a new generation of two-layer PV cells, based, for example, on nanocrystalline materials and films of conductive polymers [4,24–26]. Thus, a copper indium gallium selenide solar cell is a thin-film solar cell selected to convert sunlight into electricity because of its high conversion rate efficiency [19,27,28]. To design a long-lasting and sophisticated PV panel with a load-resistant factor design (LRFD), primarily, the uniformly distributed wind load is calculated to confirm that the PV panels are strong enough to endure heavy storms and deliver power continuously without interruptions. To confirm that PV panels are tornado-resistant (20,000 ibf > 19,375 ibf), the PV panels must have a sufficient wind load resistant capacity if the wind velocity is that of a F6 tornado (379 mile/h) at a standard air density of 1.2 kg/m^3 and with a wind pressure and drag coefficient of 1 per square meter (m^2). Since the wind stagnation pressure is half of the density of the air times the square of the velocity, Eq. (16) can be expressed as follows:

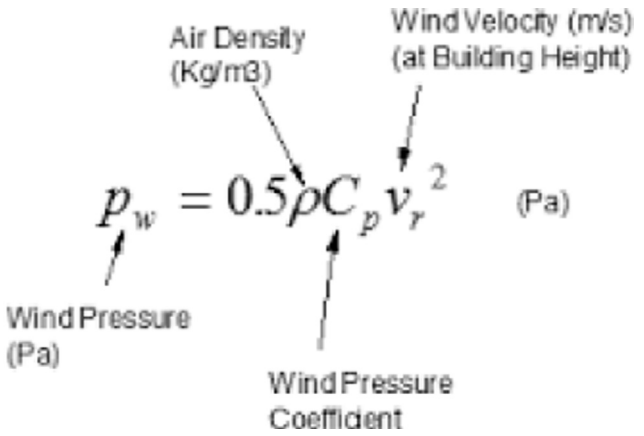

where the stagnation pressure can be determined from the following calculation: P_{ω}=0.5×1.2 kg/m^3×379^2 m/s=86,185 Pa. Finally, the wind load is calculated as F=area×drag coefficient×stagnation pressure, resulting in

$$F = 1\ \text{m}^2 \times 1.0 \times 86,185 = 86,185\ \text{N}\ (8,788\ \text{kgf} = 19,375\ \text{ibf}). \quad (17)$$

Once the wind load resistance capacity has been determined, the PV panel is analyzed to ensure that it captures the maximum amount of sunlight over the course of the entire year. The different directional angles, which can be defined using a spherical coordinate system called "horizontal coordinates," are shown in Fig. 4 and 5, where the Cartesian coordinate system uses the convention that x is south, west is y, and z is the zenith. The position of a celestial body is determined based on two angles, the height h and the azimuth angle A. Cartesian coordinates for the equatorial system use the convention that the z-axis points to the North Pole, while the y-axis (the east-west axis) is identical to the horizon system. The x-axis is perpendicular to both of the other axes. The position of a celestial body is determined by the δ declination and ω hour angles, and analysis naturally leads to the introduction of vector control strategies to control the active and reactive power based on the combination of different controls, which are reproducible and applicable to other complex systems [29–31] (Fig. 6–12).

Since the photo-physical properties are associated with the photo-induced charge [1,3], the properties of sunlight are considered by means of electromagnetic waves and momentum/photon flux impinging on a solar panel. The first view is essential for all applications of solar thermal energy and anti-reflective coatings for solar cells. The second view is essential with respect to solar cells and solar photochemistry. The unification of the two views is represented by quantum electrodynamics, one of the most fruitful and mature topics in the field of modern physics [32,33]. Although all hot bodies emit radiation, blackbodies emit the maximum amount of radiation at a temperature of approximately 700 °C, but changes in body color to orange, yellow, white, blue and efficiencies in overlapping loads have been calculated according to the band gap; the sun and cells are assumed to exhibit blackbody temperatures of 6000 K and 300 K, respectively [16]. The energy density of the radiation of the frequency can be analyzed using classical statistical physics; the maximum solar radiation occurs at 1.4 eV with an energy value of 27.77 MW/m^2 eV. This estimate is that each year an average of five levels occurs during peak hours of the day, which is the equivalent of 27,770 kW/year or 7.6 kW/day of energy.

2.3. Energy conversion by solar panels

To establish a connection between the number of light-quanta at steady state and the intensity of radiation, a finite volume enclosure containing radiation is considered [3,34]. The number of stationary states of light quanta of a certain type of polarization whose frequency is in the range of ν_r to ν_r+dν_r and maximum solar radiation can be achieved at 1.4 eV with an energy value of 27.77 MW/m^2 eV energy according to the scheme above, estimated by year based on an average of 5 h per day peak levels, which is the equivalent of 27,770 kW/year or 7.6 kW/day energy. Thus, the surface texture of selective solar metal is excellent for the purpose of energy conversion [14,35] because the current net conversion by solar panels is at a 125% higher level with an efficiency of 80% [34,36] relative to that of solar panels, corresponding to (27,770×1.25×0.8)=27,770 kW/year or 7.6 kW/day. The energy remains the same as the value before the impingement on the solar panel.

2.4. Groundwater by solar PV pumping system

Groundwater is an extremely attractive source of water for construction and homeowners, as it is available year-round and exists almost everywhere. Groundwater can be extracted by a PV solar water pumping system (SME) consisting of solar PV panels, a motor, and a pump, which is dependent on system design and requires storage, batteries, and a charge controller [7,29,36]. The engine is chosen according to the power demand and the type of current output system, which, in the case of changes in frequency and voltage imbalances, sinks backup representations and shows a promising, successful transition [18,28]. If the engine uses alternating current (AC), it must be installed using a direct current (DC)-to-AC converter. DC motors are not suitable for high-power (above 7 kW) applications in which an induction motor AC-converter AC is required [8,37]. Using an inverter will result in additional costs and energy losses. Submersible water pumps, maintenance, and replacement of DC motor brushes require the pump to be removed from the deep well, which increases operating costs and maintenance and also reduces the efficiency of solar voltaic water pumping systems (SPWPSs); without batteries, reliability and life are inexpensive, which corresponds to less maintenance relative to systems for the accumulator [31,38]. However, the storage batteries have the advantage of providing consistent performance during lean times and off-sun periods. The addition of a water storage tank in the SPWP is cheaper than backup battery storage. The use of PV solar energy is considered crucial for countries in tropical regions where direct sunlight can provide up to 1000 W/m^2. A brief analysis of the studies reporting performance, types of motors and pumps, the optimum sizing of PV panels, cooling PV solar panels, control SPWP, and economic and environmental considerations are discussed in this subsection. The Dupuit Equation (Eq. (18)) is used to calculate the pumped groundwater for the domestic water supply by a solar panel-assisted electricity supply, where h_1 and h_w are aquafer depths to the radial distances of r_1 and r_w; these variables are calculated to extract water without producing unsafe consequences such as poor water quality, large pump air compression, and water violations due to factors affecting the surroundings.

$$Q = \pi K \frac{h_1^2 - h_w^2}{\ln(r_1/r_w)} \quad (18)$$

Before the water is stored in the tank, it is treated in an in-situ water house by an activated carbon method, including disinfection, ozonation, and filtration, to ensure that the water is free from any metals or microorganisms and is 100% potable, as shown in the following diagram.

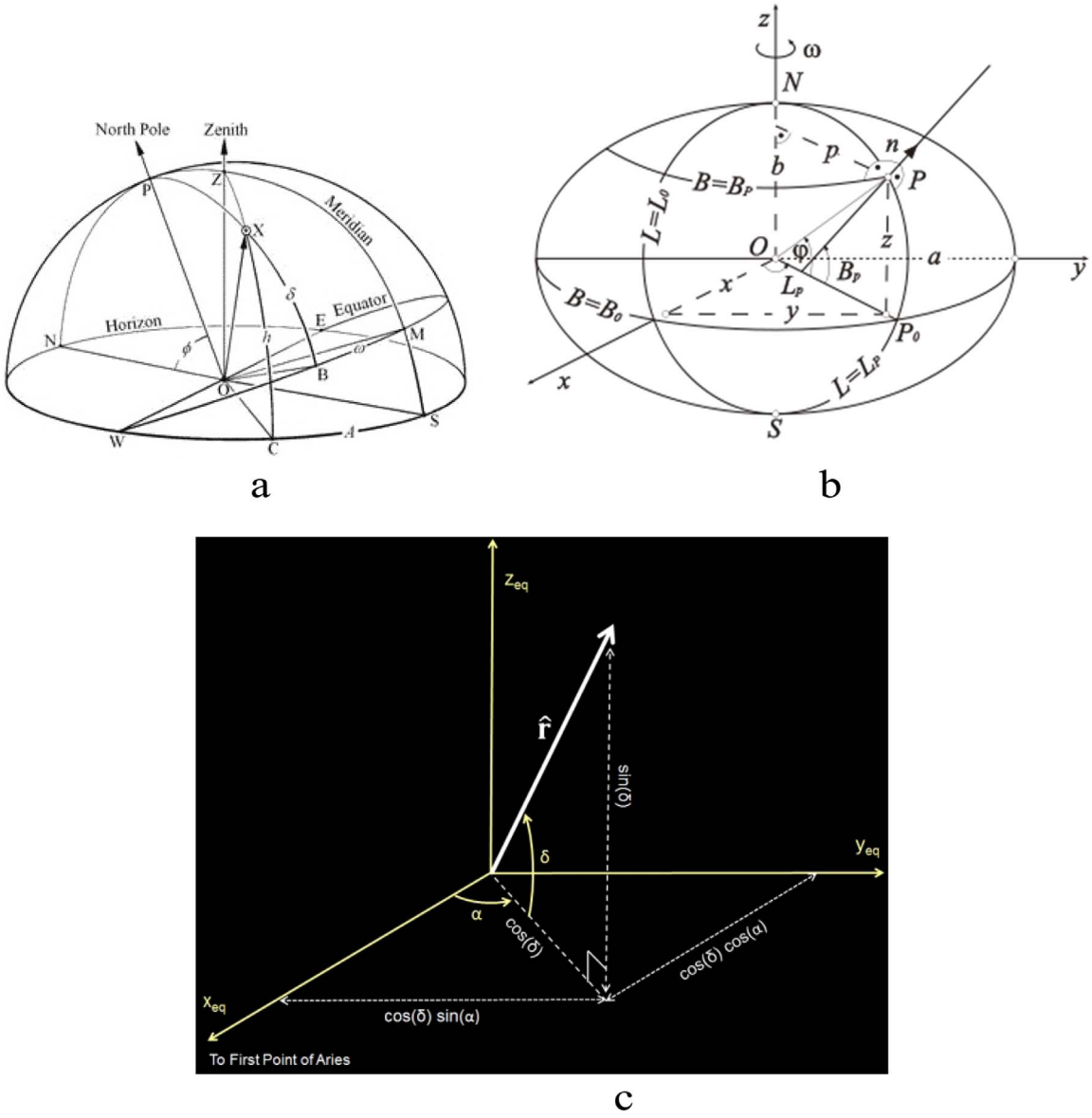

Fig. 4. (a) Cartesian coordinates analysis showing the equatorial system, (b) the position of angles, and (c) vector control considering the effect of the placement of fixed solar PV systems.
(source: adapted from [2]).

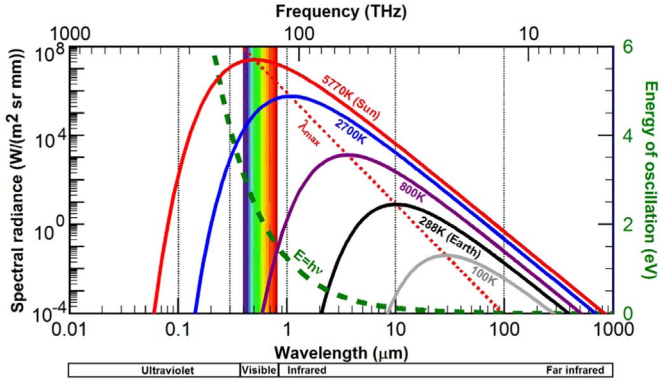

Fig. 5. The figure depicted the blackbody radiation in various temperature at 5800 K power is 6.31×10^7 (W/m^2); Peak E is 1.410 (eV); Peak λ is 0.88 (μm); Peak u is 2.81×10^7 (W/m^2 eV).
(source: [2]).

2.5. Biogas conversion from human feces and domestic waste

Interestingly, a building's solid wastewater can be collected in the closed detention tank and then separated into wastewater and feces in two different chambers. Thereafter, domestic wastewater undergoes five major processes: preliminary treatment, primary treatment, secondary treatment, disinfection, and finally, sludge treatment in-situ at the plant. The entire treatment process removes 100% of pollutants from the wastewater and disinfects the wastewater, called “effluent,” which can be used for local gardening.

Thereafter, the sludge byproduct must be treated by filtration by electrochemically-active carbon nanotubes (CNTs), which can adsorb and oxidize chemicals in the anode effectively [39]. In this study, a novel system of wastewater treatment was developed to combine both adsorption and oxidation at the anode CNT and further oxidation in-situ generated by hydrogen peroxide (H_2O_2) in the cathode CNT in a small-scale experiment. Factors that affect the efficiency of the treatment and the oxidation mechanism of the system were studied systematically. The results demonstrated that H_2O_2 flow may be

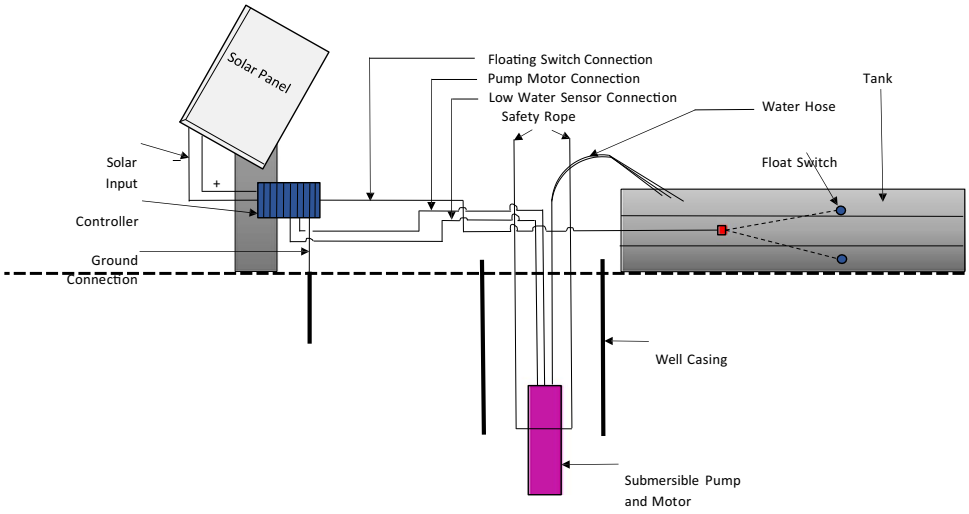

Fig. 6. Layout of solar photovoltaic water pumping system using submersible Pump. (source: adapted from [8,32]).

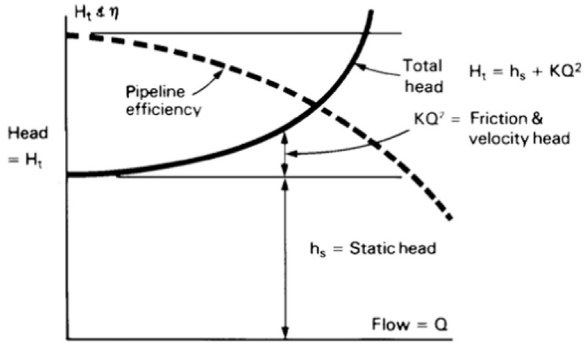

Fig. 7. The water flow capacity versus the water energy line (head) upon use of the solar PV power-assisted pump (considering the hp and efficiency of the pump) to pump groundwater.
(source: adapted from [8]).

affected by the electrode's material, the cathode potential, pH, flow rate, and the quantity of dissolved oxygen [11,21]. The maximum flow of H_2O_2 of 1.38 mol L^{-1} m^{-2} C was achieved with an applied cathodic potential voltage of −0.4 V (vs. Ag/AgCl), a pH of 6.46, a flow rate of 1.5 ml min^{-1}, and a DO influent flow of 1.95 mol L^{-1} m^{-2}. Furthermore, phenol was used as an aromatic compound model for assessing the removal efficiency of the system, and its oxidation rate correlated directly with H_2O_2 flow·H_2O_2 likely reacted with a phenol species that was anodically self-activated; H_2O_2 in its radical form cannot remove phenol efficiently. Furthermore, the formation of an electrochemical polymer through chain reactions with phenolic radicals also contributed to 13% of phenol removal. A stable removal efficiency of 87.0 ± phenol 1.8% after 4 h of continuous operation was achieved with an average rate of oxidation of 0.059 ± 0.001 mol h^{-1} m^{-2}. The electrochemical CNT filtration system developed with H_2O_2 generated in-situ is a new application of filters and carbon nanotubes; it can be used as an effective treatment for removing 100% of organic pollutants. The product can be stored in a closed chamber to allow the thermophilic anaerobic co-digestion process to cause thickening.

After thickening, the slurry is further processed to make it safer for the environment, and the sludge is placed in free-oxygen tanks called “digesters” and heated to at least 95°F for 10–15 days. This process stimulates the growth of the anaerobic bacteria *Desulfovibrio* and *Methanococcus,* which consume the organic matter in the sludge. Unlike bacteria in the aeration tanks, these bacteria thrive in a free anaerobic environment. The digestion process stabilizes the thickened sludge by converting much of the material to methane gas.

Once methanogenesis began, the organic loading rate from the following diagram on volumetric methane (biogas) production was examined by computerized gas chromatography. Biogas can be collected and stored in a biogas recovery unit and then supplied for domestic cooking fuel and the operation of HVAC equipment.

3. Results and discussion

Since fossil fuel energy resources are finite, it can be predicted using Marion King Hubbert's model that crude oil production in the world peaked in approximately 1970, then began to decline due to the shortage of fossil fuels [37,40]. His theory began with the discovery that the plots of x, the cumulative production of crude oil Q, versus y, and the ratio of the production rate P over Q for the entire world follows a straight line (Fig. 13). The two intersections of the straight line with the coordinate axes are defined as follows. The intersection with the x-axis, Q_0, is the total recoverable crude oil reserve. The value found from Fig. 13 is Q_0=228 billion barrels. The intersection with the y-axis, a, has a dimension of inverse time. The inverse of a is a measure of the duration of crude oil depletion.

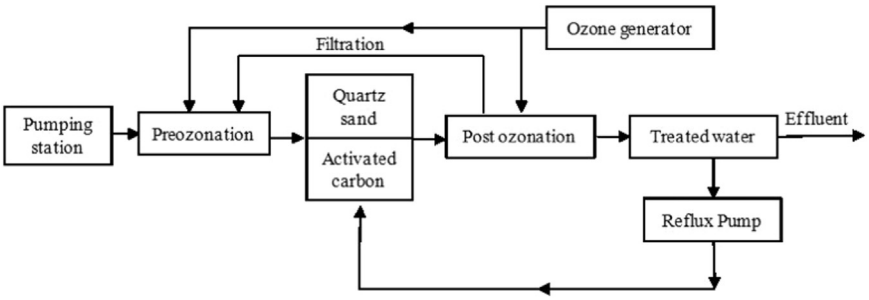

Fig. 8. The process of in situ water treatment into the water house (*Preozonation* thru effluent). (source: adapted from [8,32]).

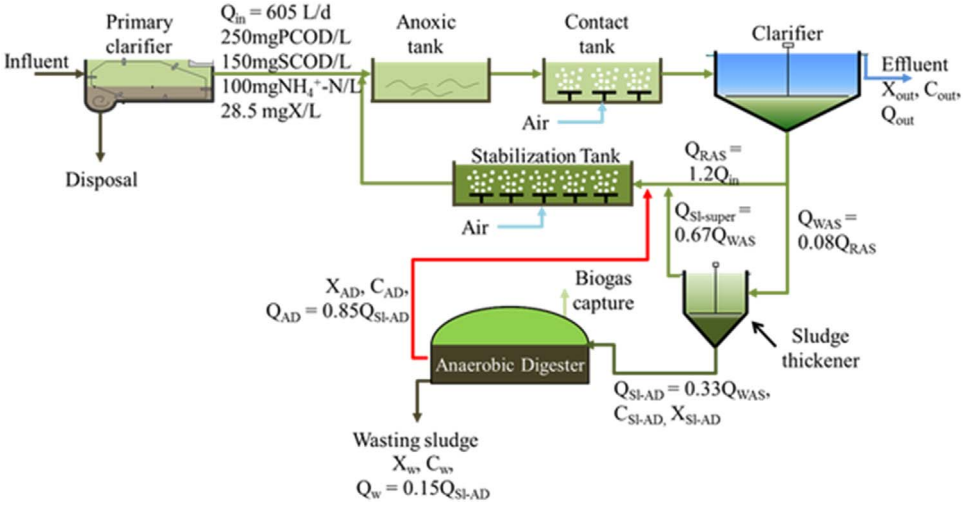

Fig. 9. A wastewater treatment process in which effluent is used for gardening and sludge is further processed to produce the biogas. (source: [44]).

One consequence of this model is that if production peaked in 1970, oil production would be expected to be in decline for the next 100 years (by 5% or less), and crude oil would be depleted in 2070. Therefore, the only option is renewable energy, in which the sun provides virtually unlimited energy for humanity; this approach can provide faster access to modern energy services anywhere in the world and access to satisfy all households' and buildings' energy demands [33,37,41]. According to the Information Administration, the average monthly electricity consumption for a residential utility consumer is approximately 903 kWh, and office and commercial buildings of 32 m×31 m with 30 m (10 floors) consume approximately 450,000 kWh in the U.S. On average, the consumption is approximately 30 kWh per day. For 5 h per day, approximately 30 kWh of energy must be generated. Therefore, the kWh divided by the hours of sunshine equals the kW required. In other words, 30 kWh/5 h of sunshine=6 kW AC output current required to cover 100% of the energy consumption. Once the AC output production value of 6 kW is known, the required quantity of solar panels can be determined. Solar panels produce DC, and houses run on AC. Due to physical limitations, there are losses in the conversion of solar energy to DC power and the conversion of DC to AC. This ratio of AC to DC is called the "derating factor," and is typically 0.8, implying that we can convert approximately 80% of DC power to AC. Therefore, we can take the quantity of AC needed, 6 kW, and divide by 0.8 (6 kW/0.8=7.5 kW DC), indicating that we will need only one 1×1 m^2 solar panel to meet the energy demand in 100% of residential houses. An office or industrial building with ten standard-sized floors would need an average of 500 1×1 m^2 solar panels SU to meet 100% of energy demand. If only 25% of the tall building's exterior skin and 25% of the ceiling were used, it would be possible to supply surplus energy to the national grid in addition to meeting the total energy demands.

Based on the maximum solar irradiance, I have calculated 1.4 eV with an energy value of 27.77 mW/m^2 eV per year in an average of 5 h/day maximum levels for 365 days reference by solar panel and

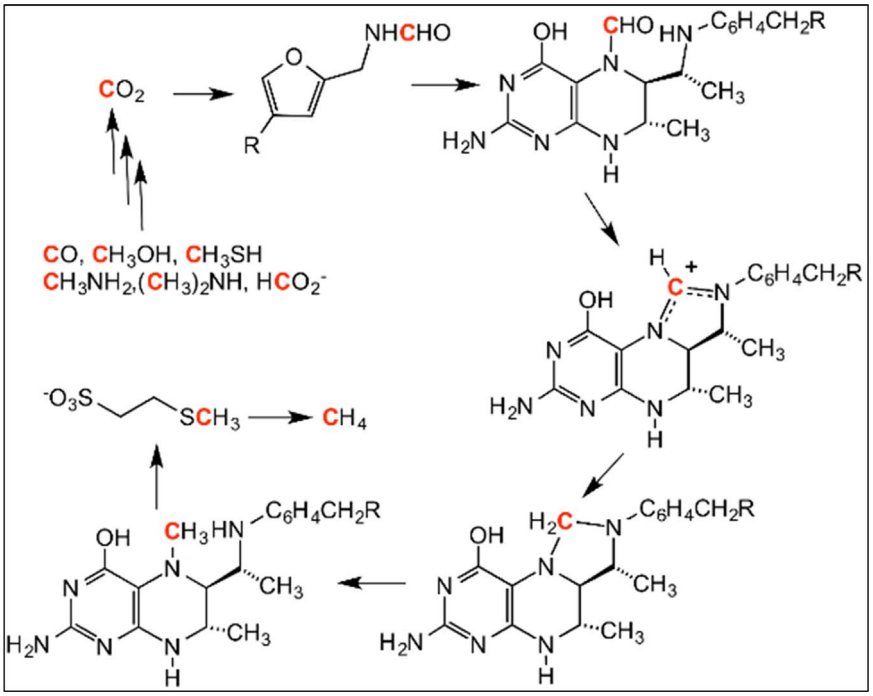

Fig. 10. Biochemical analysis of the *methanogenesis* chain reaction for producing methane. (source: adapted from [21,44]).

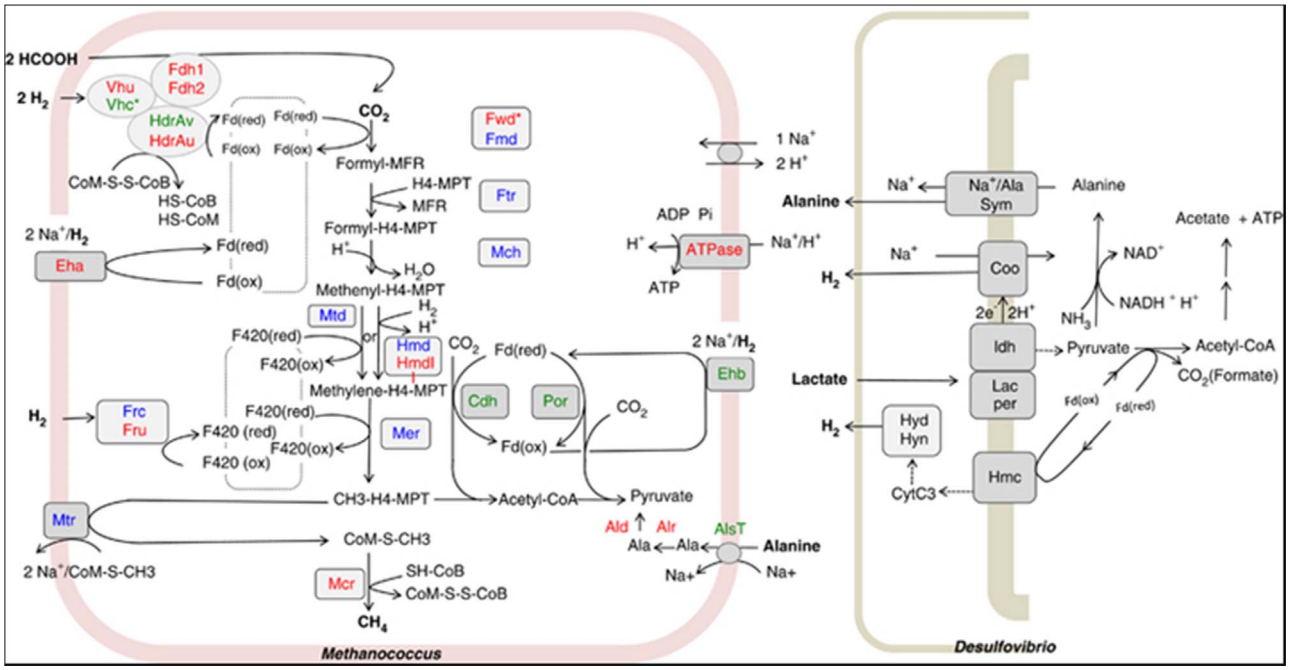

Fig. 11. Details of the methanogenesis process of bacterial syntrophic interactions between *M. maripaludis* and *D. vulgaris*, highlighting the central energy generation and consumption pathways to produce methane.
(source: adapted from [44]).

blackbody described above (Fig. 5). This energy is equivalent to 27,770 kW/year or 7.6 kW/day, which would meet the energy demands for a residential household using a solar panel with an area of 1 m^2. Since a tall building is an average of 32 m×31 m in area with a height of 30 m, a total installed panel (945+250=1195) 7.6 kW unit can provide 9082 kW/day (this is the total energy×1195). If a building's energy demand per day is 7.6 kW×500=3800 kW, additional energy of 5,282 kW/day can be supplied to the power grid to be used in other industrial sectors where the energy is required (Table 1–3).

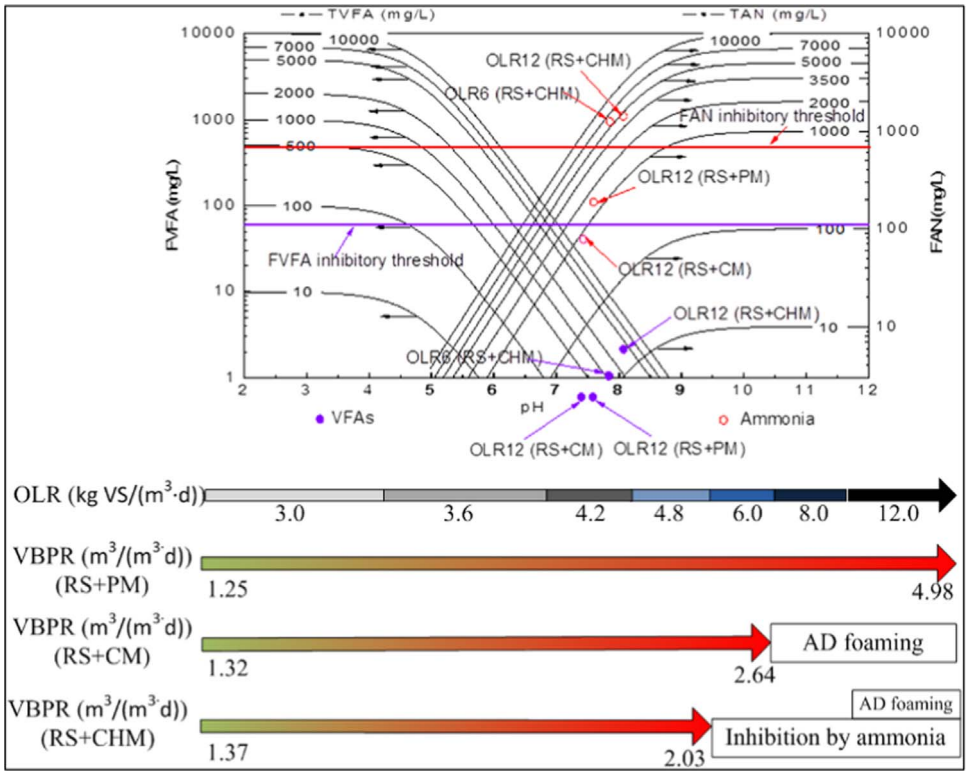

Fig. 12. Anaerobic thermophilic co-digestion of domestic perishable waste and human feces was conducted. The effects of the organic loading rate on volumetric biogas production were examined. Anaerobic digestion foaming was observed. A diagram of the inhibitory conditions of thermophilic co-digestion was plotted.
(source: adapted from [21]).

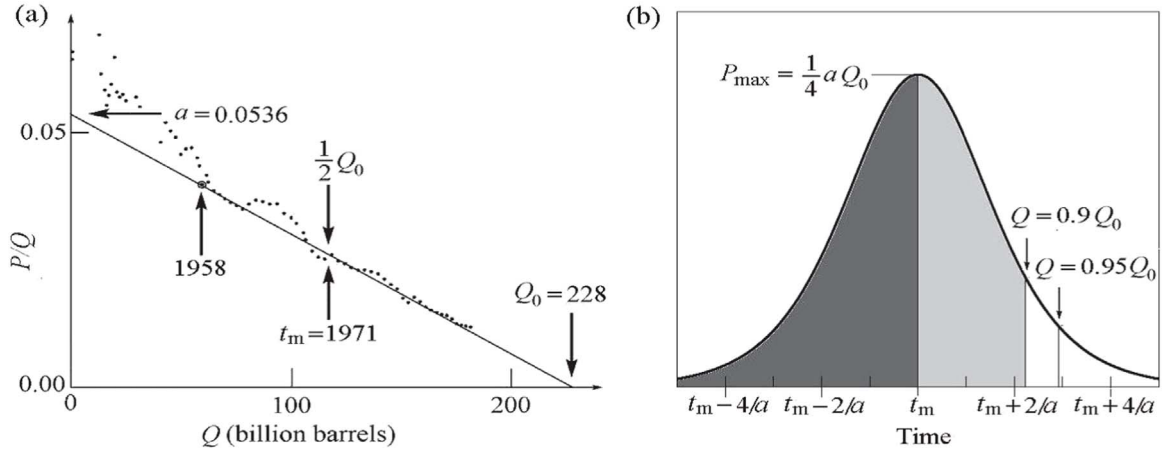

Fig. 13. (a) Shell Oil's Marion King Hubbert studied data on accumulated crude oil production, Q, and the production rate, P, worldwide. He found a linear relationship between P/Q and P. (b) The Q curve versus time can be derived from the linear relationship, the Hubbert curve. The peak of production occurs at time t_m, when half of the crude oil is depleted. At $^t m$ +2.197/a, 90% of the recoverable oil is depleted. At the time $^t m$+2.944/a, 95% of crude oil is depleted.
(source: [2]).

Table 1
This estimate (for 1195 solar panels of 1 m^2 each) was prepared by confirming the recent (June 2016) costs of materials for selected manufacturers, and the labor rate was added in accordance with the International Union of Specified Trade Workers in the U.S. The equipment rental cost is calculated based on the current rental market in conjunction with the construction standard practices' production rate.

Design and Construction Cost of the Solar Panel for Energy Production for A Ten-story Building

Component	*Material Cost*	*Labor Cost*	*Equipment Cost*	*GC & OH Cost*	*Total Cost*
Solar Panel	*$10,000*	*$5000*	*$2500*	*$3500*	*$21,000*
Instrumentation	*$2000*	*$1000*	*$2000*	*$1000*	*$6000*
Electrical, and Mechanical Control	*$2500*	*$1000*	*$1000*	*$900*	*$5400*
Supply for 30 Years cost at $0.05/kwh for monthly 4000 kWh for 100 people					*$72,000*

Total Cost $104,400

3.1. Energy cost savings

In contrast, the total cost for 30 years of energy consumption from a conventional source for a standard industry (100-person capacity) at 0.12/kWh of 4000 kWh per month is $172,800 (30×12×4000×0.12). This comparison between conventional energy use and solar panel energy *production* clearly indicates a cost savings of $68,400 when solar panels are used as the energy source.

3.2. Groundwater

Global estimates show that groundwater comprises one sixth of the total freshwater resources available in the world and is a flexible resource that can be used whenever required. Groundwater has the added benefit of incurring no losses through evaporation. Additionally, the reservoir water treatment process is highly complex and costly, and maintenance requires tremendous technical expertise and coordination between various agencies. Therefore, groundwater has emerged as an exceedingly important freshwater resource for domestic uses; it is ranked of top strategic importance because of its easy collection, and it can play an important role in mitigating climate change. An average of 100 gallons of water is required per person per day, which means that approximately 5000 gallons is required for a ten-story building (assuming 50 people/floor).

3.3. Energy cost savings

In contrast, the total cost for 30 years of water consumption from a conventional city and/or pubic department source for a standard ten-story building at 200 gallon/day/person for 50 people/floor requires 1.09×10^{10} gallons (200×50×10×30×365) of water consumption. The average cost is 0.00015/gallon of water, which is equivalent to $1,642,500 total. This comparison between conventional water use and in-situ solar panel-assisted water pumping *production and treatment* clearly indicates a cost savings of $1,259,100.

3.4. Biogas

Biogas is indeed the most significant renewable energy source because it offers an attractive and economical alternative to fossil

Table 2
This estimate was prepared by confirming recent (June 2016) costs of materials for selected manufacturers, and the labor rate was added in accordance with the International Union of Specified Trade Workers in the U.S. The equipment rental cost is calculated based on the current rental market in conjunction with the construction standard practices' production rate.

Design and Construction Cost of the Groundwater for a Ten-story Building

Component	*Material Cost*	*Labor Cost*	*Equipment Cost*	*GC & OH Cost*	*Total Cost*
Shallow Tube	*$5,000*	*$3,000*	*$2,500*	*$2,100*	*$12,600*
Filters	*$2,000*	*$1,000*	*$2,000*	*$1,000*	*$6,000*
Solar Panel Assisted Pump	*$10,500*	*$5,000*	*$1,000*	*$3,300*	*$19,800*
In-situ Treatment	*$100,000*	*$50,000*	*$100,000*	*$50,000*	*$300,000*
30 Years Maintenance cost at $1,500/year					*$45,000*

Total Cost $383,400.

Table 3
This estimate was prepared by confirming recent (June 2016) costs of materials for selected manufacturers, and the labor rate was added in accordance with the International Union of Specified Trade Workers in the U.S. The equipment rental cost is calculated based on the current rental market in conjunction with the construction standard practices' production rate.

Design and Construction Cost of Biogas Production for a Ten-story Building					
Component	***Material cost***	***Labor cost***	***Equipment cost***	***GC & OH cost***	***Total cost***
Detention Chamber	*$10,000*	*$5000*	*$2500*	*$3500*	*$21,000*
Bioreactor	*$100,000*	*$75,000*	*$50,000*	*$45,000*	*$270,000*
Electrical, and Mechanical Control	*$20,500*	*$10,000*	*$10,000*	*$8100*	*$48,600*
Gas Supply and Maintenance for 30 Years at $2000/year					*$60,000*

Total Cost $399,600.

fuels. The success of biogas production will come from its availability at low costs, its broad variety of usable forms for the production of heat, steam, electricity, and hydrogen, and its use as a household kitchen gas.

3.5. Savings on energy costs

Similarly, the total cost for 30 years of gas supply from a conventional source such as a utility company and/or agency for a standard ten-story building at $100/floor/month requires $1,800,000 (1000×50×12×30)over 30 years. This comparison between gas supplied by a conventional utility company and/or agency and on-site biogas production and supply for domestic use reveals a cost savings of $1,400,400, which is also environmentally benign.

4. Conclusions

The development of residential and commercial buildings in cities, suburban, and rural areas throughout the world has been accelerating exponentially for the past several decades [28,42]. Consequently, the dangers of climate change are increasing rapidly due to the consumption of conventional energy by the building sector [25,43]. In addition, the domestic water supplied for the buildings by extraction of reservoir water is causing severe global warming since it lowers and/or dries the water strata on Earth. Additionally, the management of city water is highly technically oriented and impacts the environment severely. Similarly, traditional wastewater management also creates severe environmental pollution, causing harm to human health and damaging aquatic fauna. Conventional sources of energy, water, and gas for buildings and houses are creating serious threats to the environment and climate. Therefore, better technology is required for the building and housing sector to create a cleaner, greener environment by deploying sustainable technology to alleviate environmental crises. Interestingly, "***Green Science***," a combined technology described above, could be the cutting-edge technology to meet the energy, water, and gas demands for buildings and houses without the need for outside connections. This sustainable technology can be used in any house and in buildings where only 25% of the exterior skin and roof will be used as the PV panel to meet its total energy demand. Naturally, PV panel power-assisted in-situ groundwater pumping and processing treatment would be implemented to meet the total domestic water consumption for buildings and houses. Subsequently, utilization of environmental pollutants (human feces and domestic waste) would be transformed into biogas by the process of *methanogenesis* to meet the buildings' and houses' total gas demand for cooking and HVAC equipment, and in-situ treated wastewater would be used for gardening and irrigation. Concerning the cost, a detailed estimate was performed to compare conventional and independent building technologies; interestingly, the results revealed that the independent building technology is much cheaper and offers better technological advantages than conventional building technology. Thus, this technology is suggested by us for maximum use globally in harvesting solar energy, in-situ groundwater pumping, and biogas production to create an independent building technology to meet all three vital needs, which indeed would be the most interesting technology in the entire world.

Funding

This research was supported by Green Globe Technology under grant RD-02016-05. Any findings, conclusions, and recommendations expressed in this paper are solely those of the author and do not necessarily reflect those of Green Globe Technology.

References

[1] Gopal C, Mohanraj M, Chandramohan P, Chandrasekar P. Renewable energy source water pumping systems—A literature review. Renew Sustain Energy Rev 2013;25:351–70.
[2] Hossain F. Solar energy integration into advanced building design for meeting energy demand and environment problem. J Energy Res 2016;17:49–55.
[3] Dirac PAM. The quantum theory of the emission and absorption of radiation. Proc R Soc A: Math Phys Eng Sci 1927;114:243–65.
[4] King R, Law D, Edmondson K, Fetzer C, Kinsey G, Yoon H, et al. 40% efficient metamorphic GaInP/GaInAs/Ge multijunction solar cells. Appl Phys Lett 2007;90:183516–900.
[5] Costa SCS, Diniz ASAC, Kazmerski LL. Dust and soiling issues and impacts relating to solar energy systems: literature review update for 2012–2015. Renew Sustain Energy Rev 2016;63:33–61.
[6] Hossain F. Wind energy modeling and its application on transporation sectors. J Energy Environ Eng 2016.
[7] Shay JL, Wagner S, Kasper HM. Efficient CuInSe2/CdS solar cells. Appl Phys Lett 2007;27:89–90.
[8] Prabhakar RJ, Ragavan K. Power management based current control technique for photovoltaic-battery assisted wind–hydro hybrid system. Int J Emerg Electr Power Syst 2013;14:351–61.
[9] Diaf S, Notton G, Belhamel M, Haddadi M, Louche A. Design and techno-economical optimization for hybrid PV/wind system under various meteorological conditions. Appl Energy 2008;85:968–87.
[10] Gelfand I, Sahajpal R, Zhang X, Izaurralde RC, Gross KL, Robertson GP. Sustainable bioenergy production from marginal lands in the US Midwest. Nature 2013;493:514–7.
[11] Ruiz HA, Martínez A, Vermerris W. Bioenergy potential, energy crops, and biofuel production in Mexico. BioEnergy Res 2016.
[12] Romero-García JM, Sanchez A, Rendón-Acosta G, Martínez-Patiño JC, Ruiz E, Magaña G, et al. An Olive tree pruning biorefinery for co-producing high value-added bioproducts and biofuels: economic and energy efficiency analysis. BioEnergy Res 2016:1–17.
[13] Grätzel M. Photoelectrochemical cells. Nature 2010.
[14] Klein SA. Calculation of flat-plate collector loss coefficients. Sol Energy 1975;17:79–80.
[15] Duan L, Sun S, Yue L, Qu W, Bian J. Study on different zero CO_2 emission IGCC systems with CO_2 capture by integrating OTM. Int J Energy Res 2016;40:1410–27.
[16] Shockley W, Queisser HJ. Detailed balance limit of efficiency of p-n junction solar cells. J Appl Phys 1961;32:510–9.
[17] Gaillard A, Poure P, Saadate S, Machmoum M. Variable speed DFIG wind energy system for power generation and harmonic current mitigation. Renew Energy 2009;34:1545–53.
[18] Kennedy CE, Price H Progress in development of high-temperature solar selective coating. In: Proceedings of the ISEC 2005, 520:36997 2005.
[19] Kamal E, Koutb M, Sobaih AA, Abozalam B. An intelligent maximum power extraction algorithm for hybrid wind–diesel-storage system. Int J Electr Power Energy Syst 2010;32:170–7.
[20] Bhandari B, Poudel SR, Lee K-T, Ahn S-H. Mathematical modeling of hybrid renewable energy system: a review on small hydro-solar-wind power generation. Int J Precis Eng Manuf-Green Technol 2014;1:157–73.
[21] Liu Y, Xie J, Ong CN, Vecitis CD, Zhou Z. Electrochemical wastewater treatment with carbon nanotube filters coupled with in situ generated H_2O_2. Environ Sci: Water Res Technol 2015;1:769–78.
[22] Born M, Wolf E. Principles of Optics. Cambridge: Cambridge University Press; 1999.

[23] Green MA. Limits on the open-circuit voltage and efficiency of silicon solar cells imposed by intrinsic Auger processes. IEEE Trans Electron Devices 1996;31:671–8.
[24] Gratzel M. Photoelectrochemical cells. Nature 2001;414:338–44.
[25] Stix M. The Sun, an Introduction, 2nd ed.. New York: Springer; 2002.
[26] Tang CW. Two-layer organic photovoltaic cell. Appl Phys Lett, 48: pp. 183–85.
[27] Liu BYH, Jordan RC. The interrelationship and characteristic distribution of direct, diffuse and total solar radiation. Sol Energy 1960;4:1–19.
[28] Brabec CJ, Sariciftci NS, Hummelen JC. Plastic solar cells. Adv Funct Mater 2001;11:15–26.
[29] ASAC Diniz, LVBM Neto, Camara , Morais CF, Cabral P, Filho CVT. DO, et al. Review of the photovoltaic energy program in the state of Minas Gerais, Brazil. Renew Sustain Energy Rev 2011;15:2696–706.
[30] Dürr M, Cruden A, Gair S, McDonald JR. Dynamic model of a lead acid battery for use in a domestic fuel cell system. J Power Sources 2006;161:1400–11.
[31] Mamdani EH, Assilian S. An experiment in linguistic synthesis with a fuzzy logic controller. Int J Man-Mach Stud 1975;7:1–13.
[32] Maxwell J, Torrance TF. A Dynamical Theory of the Electromagnetic Field. Oregon: Wipf & Stock Publishers; 1996.
[33] Beatty JK, Peterson CC, Chaokin A. The Solar System. Cambridge, UK: Cambridge University Press; 1999.
[34] Bethe HA. Energy production in stars. Phys Rev 1939;55:434–56.
[35] Millikan RA. A direct photoelectric determination of Planck's" h". Phys Rev 1916;7:355.
[36] Hossain MF. *In situ* geothermal energy technology: an approach for building cleaner and greener environment. J Ecol Eng 2016;17:49–55.
[37] Nema P, Nema RK, Rangnekar S. A current and future state of art development of hybrid energy system using wind and PV-solar: a review. Renew Sustain Energy Rev 2009;13:2096–103.
[38] Zhao J, Wang A, Altermatt PP, Wenham SR, Green MA. 24% efficient perl silicon solar cell: recent improvements in high efficiency silicon cell research. Sol Energy Mater Sol Cells 1996;41:87–99.
[39] Anish Modi, Bühler Fabian, Andreasen Jesper Graa, Haglind Fredrik. A review of solar energy based heat and power generation systems. Renew Sustain Energy Rev 2017;67:1047–64.
[40] Kennedy C. Reiew of mid- to high-temperature absorber materials. Natl Renew Energy Lab Rep 2002;520:31267.
[41] Kane M. Small hybrid solar power system. Energy 2003;28:1427–43.
[42] Mohd Zin AAB, Pesaran HAM, Khairuddin AB, Jahanshaloo L, Shariati O. An overview on doubly fed induction generators′ controls and contributions to wind based electricity generation. Renew Sustain Energy Rev 2013;27:692–708.
[43] Agarwal V, Aggarwal RK, Patidar P, Patki C. A novel scheme for rapid tracking of maximum power point in wind energy generation systems. IEEE Trans Energy Convers 2010;25:228–36.
[44] Chena Huihui, Wana Jingjing, Chena Kaifei, Luoa Gang, Fanb Jiajun, Clarkb James, Zhanga Shicheng. Biogas production from hydrothermal liquefaction wastewater (HTLWW): focusing on the microbial communities as revealed by high-throughput sequencing of full-length 16S rRNA genes. Water Res 2016;06:98–107.